available at www.sciencedirect.com

ScienceDirect

journal homepage: www.elsevier.com/locate/chnjc

Article (Special Issue on Photocatalysis in China)

Photocatalytic Cr(VI) reduction and organic-pollutant degradation in a stable 2D coordination polymer

Fu-Xue Wang [a], Xiao-Hong Yi [a], Chong-Chen Wang [a,*], Ji-Guang Deng [b,#]

[a] *Beijing Key Laboratory of Functional Materials for Building Structure and Environment Remediation/Sino-Dutch R&D Centre for Future Wastewater Treatment Technologies, Beijing University of Civil Engineering and Architecture, Beijing 100044, China*

[b] *Department of Chemistry and Chemical Engineering, College of Environmental and Energy Engineering, Beijing University of Technology, Beijing 100022, China*

ARTICLE INFO

Article history:
Received 4 October 2017
Accepted 26 October 2017
Published 5 December 2017

Keywords:
Photocatalysis
Cr(VI) reduction
Organic dyes
Coordination polymers
Degradation

ABSTRACT

A new coordination polymer, Zn(bpy)L (**BUC-21**), (H_2L = *cis*-1,3-dibenzyl-2-imidazolidone-4,5-dicarboxylic acid, bpy = 4,4′-bipyridine), has been synthesized under hydrothermal conditions, and characterized by single-crystal X-ray analysis, Fourier transform infrared spectroscopy, thermogravimetric analyses, CNH elemental analysis and UV-Vis diffuse reflectance spectroscopy. **BUC-21** exhibited an excellent performance for photocatalytic Cr(VI) reduction with a conversion efficiency of 96%, better than that of commercial P25 (39%), under UV light irradiation for 30 min. **BUC-21** could also be used to conduct photocatalytic degradation of organic dyes including methylene blue, rhodamine B, methyl orange and reactive red X-3B. Also, the photocatalytic activity of **BUC-21** remained high across a wide pH range from 2.0 to 12.0. It is interesting to note, however, that **BUC-21** was unable to achieve simultaneous reduction of Cr(VI) and degradation of an organic pollutant in a mixed matrix, which can be attributed to the competition between Cr(VI) and the organic dyes for access to the photo-excited electrons.

1. Introduction

In recent years, industrial activity has generated large amounts of wastewater, which often contains high concentrations of organic pollutants and inorganic heavy metal ions. Among the heavy metal ions, one of the most common contaminants is Cr(VI), which has been classified as a carcinogen and mutagen because of its high toxicity and harmfulness to most organisms, including humans [1–3]. Although Cr(VI) can be removed from aquatic environments by adsorption [4], it still poses a risk through secondary pollution. Cr(III), however, is low-toxic and even beneficial to living organisms, and is also easily precipitated or adsorbed on inorganic/organic substrates at neutral or alkaline pH [5,6]. Therefore, it is environmentally beneficial to deoxidize Cr(VI) to Cr(III). Another class of aquatic contaminants is organic dye molecules, which usually contain benzene rings, making them hard to degrade by conventional chemical and biological methods [7]. Discharging of dyes into aquatic environments, even in small amounts, can pose severe risks to human health [8].

* Corresponding author. Tel/Fax: +86-10-61209186; E-mail: chongchenwang@126.com
# Corresponding author. E-mail: jgdeng@bjut.edu.cn

This work was supported by the National Natural Science Foundation of China (51578034), the Beijing Natural Science Foundation & Scientific Research Key Program of Beijing Municipal Commission of Education (KZ201410016018), Beijing Talent Project (2016023), and Project of Construction of Innovative Teams and Teacher Career Development for Universities and Colleges Under Beijing Municipality (IDHT20170508).
DOI: 10.1016/S1872-2067(17)62947-4 | http://www.sciencedirect.com/science/journal/18722067 | Chin. J. Catal., Vol. 38, No. 12, December 2017

Photocatalysis is a potential technology for carrying out Cr(VI) reduction [9], which is more effective and lower in cost compared with other methods like electro-reduction [10–12] and chemical reduction [13–15]. Meanwhile, photocatalysis can also be used to decompose organic pollutants into biodegradable or less toxic compounds, or even into inorganic CO_2, H_2O, NO_3^- and halide ions [7,16]. TiO_2 has been reported as an effective photocatalyst for these reactions because of its high activity, low toxicity, low cost and good stability and durability [17–19], although it suffers from low photocurrent quantum yield, difficult post-separation and the tendency toward agglomeration [20,21]. CdS, SnS_2 and WO_3 have been used as photocatalysts under visible light irradiation [22–30], but their effectiveness was limited by their poor efficiency and slow rate [31]. Consequently, it has become urgent to find new efficient photocatalysts for the reduction of Cr(VI) and degradation of organic pollutants.

Coordination polymers (CPs) have gained much attention for their fascinating architectures and potential applications in photocatalysis [7,32], conventional catalysis [33,34], separation [35,36], CO_2 capture [37,38], gas storage [39,40], pollutant adsorption [41,42] and other processes [43–45]. Because of the catalytically active metal sites and the synergistic effects of the metals with functional organic ligands, along with the large surface area and permanent pores, CPs show great potential opportunities for heterogeneous photocatalysis, including H_2 production, Cr(VI) reduction and organic-pollutant degradation [46–50]. Zhao et al. [51] reported the reduction of Cr(VI) with high efficiency by NNU-36 ($[Zn_2(BPEA)(BPDC)_2]\cdot 2DMF$). Shen et al. [52] demonstrated that the Pd@UiO-66(NH_2) nanocomposite exhibited excellent photocatalytic reduction of Cr(VI), and even showed enhanced activity in a binary system of Cr(VI) and organic dyes. Wang et al. [53] developed ZnO@ZIF-8 core-shell heterostructures, which were utilized to perform selective photoreduction of Cr(VI) from mixed Cr(VI)/MB solution (MB = methylene blue). Besides these 3D materials, 2D layered materials and their composite photocatalysts also have many unique properties, such as tunable band gaps, which can enhance their photocatalytic performance [54–56]. In summary, these previous reports revealed the potential application of photocatalysts based on CPs (including metal–organic frameworks, MOFs) to reduce Cr(VI) to Cr(III) and degrade organic pollutants in wastewater.

Herein, the primary ligand 1,3-dibenzyl-2-imidazolidone-4,5-dicarboxylic acid (H_2L) and the secondary ligand rigid 4,4′-bipyridine (bpy) were selected to construct a new CP, Zn(bpy)L (named **BUC-21**). To the best of our knowledge, this is the first use of H_2L as a linker to build a CP. The current work demonstrates that **BUC-21** exhibits an excellent reusability and much higher Cr(VI) reduction efficiency and reduction rate than those of P25 under the same conditions. Meanwhile, **BUC-21** shows high photocatalytic activities for degradation of organic dyes, including cationic methylene blue (MB) and rhodamine B (RhB) and anionic methyl orange (MO) and reactive red X-3B (X-3B). In a matrix system containing both Cr(VI) and an organic dye, however, both the Cr(VI) reduction rate and the organic-pollutant degradation rate are decreased. A possible mechanism for this effect is proposed.

2. Experimental

2.1. Preparation

All commercially available chemicals were reagent grade, and used as received without further purification. Fourier transform infrared (FTIR) spectra were recorded in the region ranging from 4000 to 400 cm^{-1} on a Nicolet 6700 infrared spectrophotometer with KBr pellets. Thermogravimetric analyses (TGA) were performed from 80 to 800 °C in an air stream at a heating rate of 10 °C min^{-1} on a DTU-3c thermal analyzer using α-Al_2O_3 as reference. Ultraviolet-visible (UV-vis) diffuse reflectance spectra of solid samples were measured by a PerkinElmer Lambda 650S spectrophotometer, in which $BaSO_4$ was used as the standard with 100% reflectance.

2.2. Synthesis of *BUC-21*

A mixture of $ZnCl_2$ (0.3 mmol, 40.89 mg), bpy (0.3 mmol, 46.85 mg) and H_2L (0.3 mmol, 106.31 mg) was sealed in a 25 mL Teflon-lined stainless steel Parr bomb containing deionized H_2O (18 mL), heated at 160 °C for 72 h, and cooled down slowly to room temperature. White block-like crystals of $C_{29}H_{24}N_4O_5Zn$ (**BUC-21**, yield 82% based on $ZnCl_2$) were isolated and washed with deionized water. Anal. Calcd. for **BUC-21**, $C_{29}H_{24}N_4O_5Zn$: C, 60.6%; N, 9.8%; H, 4.2%. Found: C, 60.8%; N, 9.9%; H, 4.3%. FTIR (KBr)/cm^{-1}: 3575, 3434, 3057, 2920, 2861, 2463, 1961, 1645, 1536, 1493, 1417, 1281, 1220, 1141, 1070, 1047, 1033, 1015, 965, 949, 915, 860, 813, 762, 745, 726, 703, 673, 643, 619, 570, 519, 484.

2.3. X-ray crystallography

X-ray single-crystal data collection for **BUC-21** was carried out with a Bruker CCD area detector diffractometer with graphite-monochromatized Mo K_α radiation (λ = 0.71073 Å) using the φ-ω mode at 298(2) K. The SMART software [57] was used for data collection and the SAINT software [58] for data extraction. Empirical absorption correction was performed with the SADABS program [59]. The structure was solved by direct methods (SHELXS-97) [60] and refined by full-matrix-least squares techniques on F^2 with anisotropic thermal parameters for all of the non-hydrogen atoms (SHELEL-97) [60]. All hydrogen atoms were located by Fourier difference synthesis and geometrical analysis. These hydrogen atoms were allowed to ride on their respective parent atoms. All structural calculations were carried out using the SHELX-97 program package [60]. Crystallographic data and structural refinement for **BUC-21** are summarized in Table S1. Selected bond lengths and angles are listed in Table S2.

2.4. Evaluation of photocatalytic activity

The working electrode was prepared on a fluorine-doped tin oxide (FTO) glass, which was cleaned by sonication in etha-

nol for 15 min, and then dried under air. The FTO slide was dip-coated with 10 μL of slurry, which was obtained by mixing 5.0 mg **BUC-21** powder (with particle sizes less than 0.074 mm) and 0.3 mL ethanol under sonication for 2 h. During dip-coating, the side part of the FTO slide was protected using Scotch tape. A copper wire was connected to the side part of the FTO glass using conductive tape. The uncoated parts of the electrode were isolated with an epoxy resin, and the exposed area of the electrode was about 0.25 cm^2. The electrochemical measurements were performed in a conventional three-electrode cell, using a Pt plate as counter electrode and a saturated Ag/AgCl electrode as reference electrode. Before measurement, the working electrodes were immersed in a Na_2SO_4 aqueous solution (0.2 mol L^{-1}) for 30 s. The photocurrents were measured with a Metrohm PGSTAT204 workstation. A UV lamp with optical power efficiency of 142 mW cm^{-2} (Beijing Perfectlight Co. Ltd.) was used as a light source.

2.5. Photocatalytic tests

The photocatalytic experiments for Cr(VI) reduction from $K_2Cr_2O_7$ aqueous solution were conducted at ambient conditions in a quartz reactor containing 15.0 mg photocatalyst and 200 mL of 10 mg L^{-1} Cr(VI) solution. After stirring for 30 min to reach adsorption-desorption equilibrium, the suspensions were irradiated by a 500-W Hg lamp (Beijing Aulight Co., Ltd). During the photocatalytic degradation experiments, 1.5 mL aliquots were extracted at 3 min intervals for analysis. The Cr(VI) content in the supernatant was determined colorimetrically at 540 nm using the diphenylcarbazide (DPC) method. Additionally, two cationic organic dyes, MB (10 mg L^{-1}) and RhB (10 mg L^{-1}), and two anionic organic dyes, MO (10 mg L^{-1}) and X-3B (50 mg L^{-1}), were selected as organic pollutant models to evaluate the photocatalytic performances of **BUC-21** under the same conditions. A Laspec Alpha-1860 spectrometer was used to monitor the concentration changes determined at the maximum absorbance of 664, 554, 463 and 540 nm for MB, RhB, MO and X-3B, respectively.

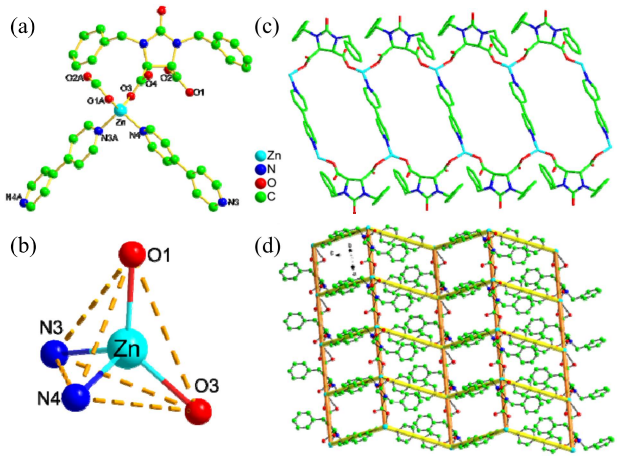

Fig. 1. (a) Asymmetric unit of **BUC-21**; (b) Coordination polyhedron for Zn(II) atoms; (c) 2D network and (d) Packing diagram for **BUC-21** (orange sticks and yellow sticks represent L and bpy, respectively).

3. Results and discussion

3.1. Crystallographic structure analyses

The crystal structure analysis revealed that the asymmetric unit of Zn(bpy)L is built up of one Zn(II) atom, two bpy ligands and two monodentate bridging carboxylate groups from two different L^{2-} groups (Fig. 1(a)). The Zn-N and Zn-O distances are in the range of 2.049–2.050 Å and 1.928(4)–1.959(5) Å, respectively, which are comparable to previously reported values [61]. The Zn(II) atoms, adopting tetrahedral geometries as illustrated in Fig. 1(b), are linked into 1D chains by completely deprotonated L^{2-} groups along the *a*-axis, which are further joined into a 2D framework by rigid bpy ligands, as shown in Fig. 1(c) and (d).

3.2. Characterization

BUC-21 was stable under air, and stable and insoluble in water and common organic solvents, including ethanol, methylbenzene, chloroform, ether, DMSO and DMF. The FTIR spectrum of **BUC-21** was recorded, and as depicted in Fig. S1, the band at 2861 cm^{-1} can be assigned to ν(-CH_2-) vibrations [62]. The strong and broad bands at 1645 and 1417 cm^{-1} are ascribed to the asymmetric and symmetric vibrations, respectively, of carboxyl groups. The bands at 1220 and 1141 cm^{-1} can be assigned to the ν(C-N) vibrations of the phenyl rings. The thermal stability of **BUC-21** was examined by TGA, which established that the framework of **BUC-21** was stable up to 340 °C (Fig. S2). The optical properties of **BUC-21** were investigated by UV-vis diffuse reflectance spectrophotometry (UV-vis DRS). As shown in Fig. 2, the sample absorbed light in the UV region. The band gap (E_g) value was estimated using the Kubelka-Munk function, $F = (1 - R)^2/2R$ [63], where R is the reflectance of an infinitely thick layer at a given wavelength. The F versus E plot is shown in Fig. 2 (inset), where a steep absorption edge is displayed and the E_g value of the sample can be assessed at 3.4 eV, implying that **BUC-21** is a potential wide-gap photocatalyst [64,65].

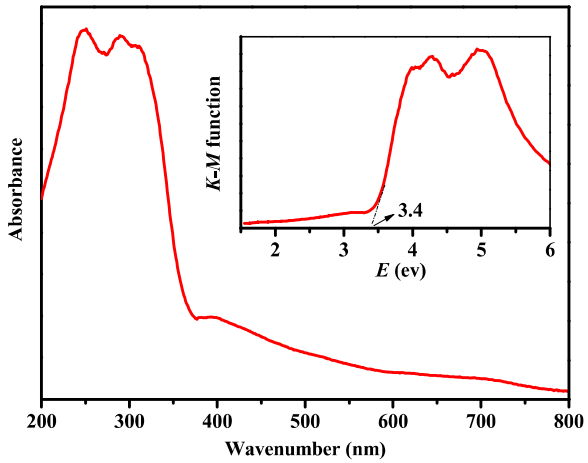

Fig. 2. UV-vis spectrum of **BUC-21.** The inset shows the Kubelka-Munk-transformed diffuse reflectance spectrum of **BUC-21.**

3.3. Photocatalytic performance

Previous studies have shown that the reduction rate of aqueous Cr(VI) over photocatalysts is greatly influenced by the pH values [2,52]. Theoretically, the $Cr_2O_7^{2-}$ anion is predominant in solution under acidic conditions. To obtain the optimum reaction conditions, controlled experiments were first carried out with the addition of different amounts of H_2SO_4 solution (1:1, *v*/*v*). As shown in Fig. 3, the pH greatly influenced the photocatalytic activity of **BUC-21**. As the pH was successively decreased from 4.0 to 2.0, the reduction rate of Cr(VI) markedly increased. At pH = 1, however, the photocatalytic activity was significantly lower than at pH = 2 or 3, possibly because of destruction of the framework of **BUC-21** (Fig. S3). The efficiency of photocatalytic Cr(VI) reduction was even poorer under alkaline conditions (not shown). As mentioned above, the predominating species of Cr at pH 2–4 is $Cr_2O_7^{2-}$ [52,66]. Therefore, the proposed reactions may be described by Eqs. (1) and (2):

$$\textbf{BUC-21} + h\nu \rightarrow \textbf{BUC-21}\ (e^- + h^+) \quad (1)$$

$$Cr_2O_7^{2-} + 14H^+ + 6e^- \rightarrow 2Cr^{3+} + 7H_2O \quad (2)$$

The Cr(VI) reduction efficiencies of H_2L, **BUC-21** and commercial P25 under UV light irradiation are shown in Fig. 4. About 39% and 59% of the initial content of Cr(VI) was deoxidized after 30 min in the presence of P25 and H_2L as photocatalysts, respectively. In comparison, the reduction rate was significantly increased in the presence of **BUC-21**, which achieved a reduction efficiency of 96% within 30 min. The extent of Cr(VI) reduction was minimal in the absence of photocatalyst or light, implying that the removal of Cr(VI) could be classified as a photocatalytic process.

To further characterize the photocatalytic behavior of **BUC-21**, four organic dyes (MB, RhB, MO and X-3B) were selected to perform degradation experiments under UV light irradiation. For comparison, control experiments were conducted in two different systems, under identical conditions to the main experiments except for the absence of light (but presence of photocatalysts) in one system, and the absence of photocatalyst (but presence of UV irradiation) in the other. The adsorptive removal rates of the four selected organic dyes in the presence of **BUC-21** in the dark were negligible, as shown in Fig. 5. In the absence of any photocatalyst, ca. 20% MB, 16% RhB, 15% MO and 53% X-3B were decomposed after 30 min UV irradiation, and with the H_2L ligand as photocatalyst, 61% X-3B was decomposed. In comparison, **BUC-21** exhibited outstanding UV-photocatalytic activities, degrading 93% MB, 97% MO and 100% X-3B in 30 min. These photocatalytic activities of **BUC-21** are much higher than those in previous reports [67–71]. Besides, it should be noted that X-3B was completely removed by **BUC-21** within only 9 min, which was faster than the time required by P25 (24 min) under the same conditions. A comparison of the performance of **BUC-21** with those of previous 2D catalysts is listed in Table 1.

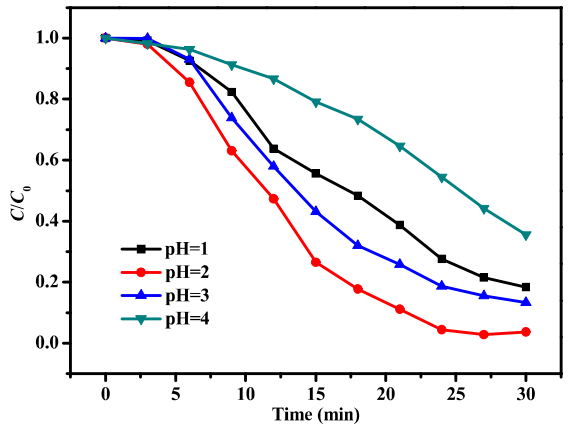

Fig. 3. Photocatalytic Cr(VI) reduction over **BUC-21** under UV light irradiation at different pH.

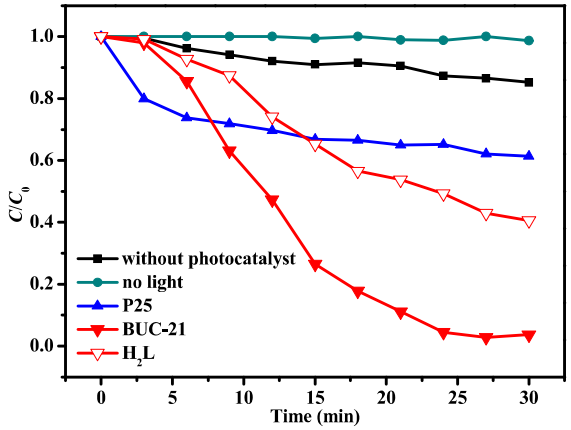

Fig. 4. Photocatalytic reduction of Cr(VI). Reaction conditions: 15 mg photocatalyst, 200 mL Cr(VI) (10 mg L^{-1}), pH = 2.0.

Furthermore, the photocatalytic activity of **BUC-21** for simultaneous Cr(VI) reduction and dye degradation in a Cr(VI)/dye mixed system was investigated at pH = 2.0. As displayed in Fig. 6, for the mono-component systems, the Cr(VI) reduction and X-3B degradation efficiencies were 96% and 100%, respectively, within only 15 min. In the Cr(VI)/dye mixed system, the efficiency of Cr(VI) reduction was still ca. 96%. However, the removal percentage of X-3B was significantly decreased to 68%. It is well known that both holes (h^+)

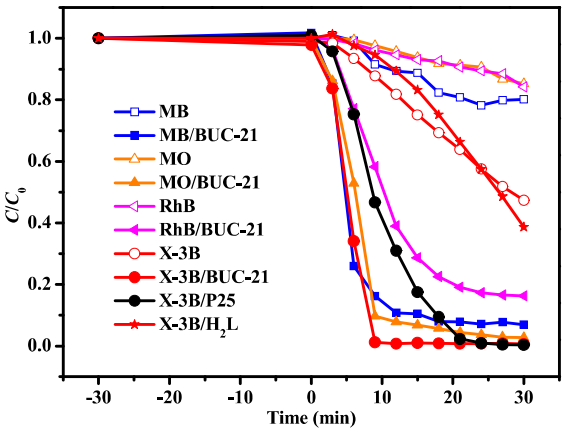

Fig. 5. Photocatalytic degradation of MB, RhB, MO and X-3B solution by **BUC-21**. Experimental conditions: 15 mg photocatalyst, 200 mL of 10 mg L^{-1} MB, RhB, MO, 50 mg L^{-1} X-3B. Initial pH: MB 7.7, MO 7.6, RhB 6.8, X-3B 4.3.

Table 1
Comparison of the photocatalytic performances of various 2D photocatalysts.

Catalyst/mg	Pollutants/mg L^{-1}	Irrigation	Time/min	Efficiency (%)	Ref.
ZnO/50	MO/20	UV	540	8	[72]
$[Zn(L)(bpy)CH_3CN]_n$/50	RhB/10	UV	100	29	[73]
BiOBr/50	RhB/30	vis	1500	92	[74]
Ni(bismip)(bpy)$(H_2O)_2$/40	MB/10	UV	180	80	[75]
N-$K_2Ti_4O_9$/UiO-66-NH_2/20	MB/5	vis	180	92	[76]
g-C_3N_4/MIL-53(Fe)/20	Cr(VI)/10	vis	180	100	[48]
g-C_3N_4/30	Cr(VI)/10	vis	180	5	[77]
Co-TNSs/100	Cr(VI)/50	vis	140	70	[30]

L = 5-aminoisophthalic acid; bismip = 5-(1*H*-benzoimidazol-2-ylsulfanylmethyl)-isophthalic acid; TNSs: CoO_x-loaded TiO_2-based nanosheets.

and electrons (e^-) are produced in a photocatalyst under light irradiation. Cr(VI) is reduced to Cr(III) by e^-, while many dyes can be oxidized by h^+ [52,78]. On this basis, one would expect both the reduction of Cr(VI) and degradation of X-3B to be enhanced in the mixed system. Instead, the photocatalytic degradation of X-3B was decreased, and the reduction of Cr(VI) was not improved. To explain this observation, we propose that the X-3B was not oxidized by the holes but by $\cdot O_2^-$ radical anions, which were generated by the reaction of e^- and O_2. In the mixed system, the e^- were consumed by Cr(VI), resulting in the decreased rate of X-3B degradation.

To prove the assumption that the X-3B was photocatalytically degraded by $\cdot O_2^-$, benzoquinone (BQ) was introduced as a scavenging agent to trap $\cdot O_2^-$. In a separate experiment, the potential role of ·OH radicals was also investigated by adding isopropyl alcohol (IPA). The concentrations of both BQ and IPA were 0.2 mmol L^{-1}. As shown in Fig. 7, the X-3B degradation rate was significantly restrained in the presence of BQ, which suppresses $\cdot O_2^-$ activity. Although the degradation proceeded at a steady rate, the removal percentage was down to 51%. However, when IPA was added instead, as an ·OH scavenger, X-3B was completely degraded within 24 min, suggesting that ·OH was not the dominant active species involved in the degradation. It can be concluded that $\cdot O_2^-$ was the main active species, and ·OH was secondary, while the holes played no significant role in this photocatalytic reaction.

It can be seen from the above experiments that **BUC-21** exhibited high photocatalytic activities towards Cr(VI) and organic pollutants in acidic and neutral solutions. In a further set of experiments, a solution of X-3B (initial pH = 4.3) was selected to study the photocatalytic activity of **BUC-21** in alkaline conditions. As the pH value was successively increased from 6 to 12, the photocatalytic efficiency of X-3B degradation was markedly improved (Fig. 8). This relationship between the degradation rate of X-3B and the pH of the solution may be related to either the protonation/deprotonation of the basic

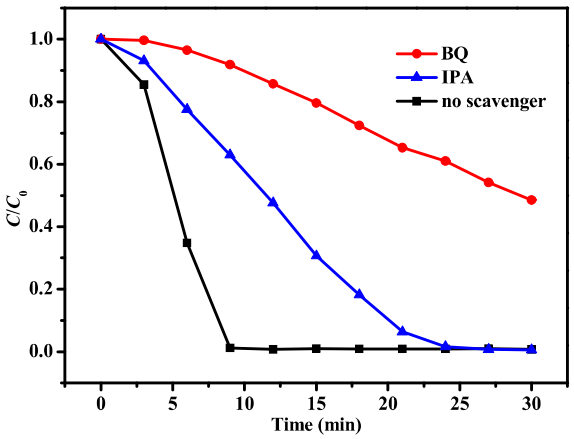

Fig. 7. Effects of different scavengers on degradation of X-3B in the presence of **BUC-21.** Reaction conditions: 15 mg **BUC-21**, 200 mL of X-3B (50 mg L^{-1}), 0.2 mmol L^{-1} scavengers.

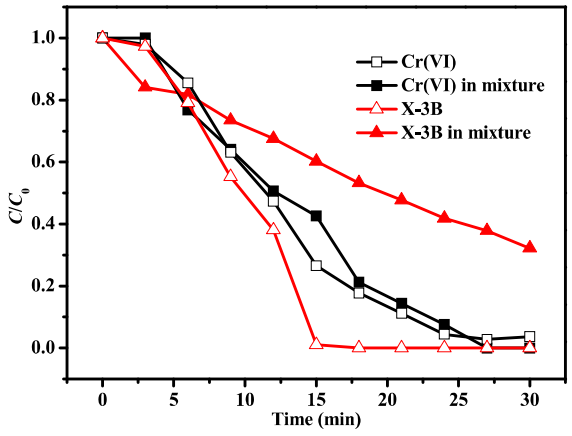

Fig. 6. Photocatalytic reduction of Cr(VI) and degradation of X-3B in single systems and in mixed system. Reaction conditions: 15 mg **BUC-21**, 200 mL of Cr(VI) (10 mg L^{-1}) and X-3B (50 mg L^{-1}), pH = 2.0.

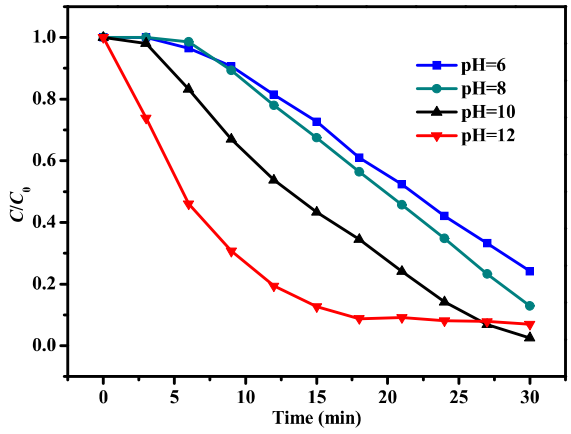

Fig. 8. Degradation of X-3B over **BUC-21** under neutral and alkaline conditions.

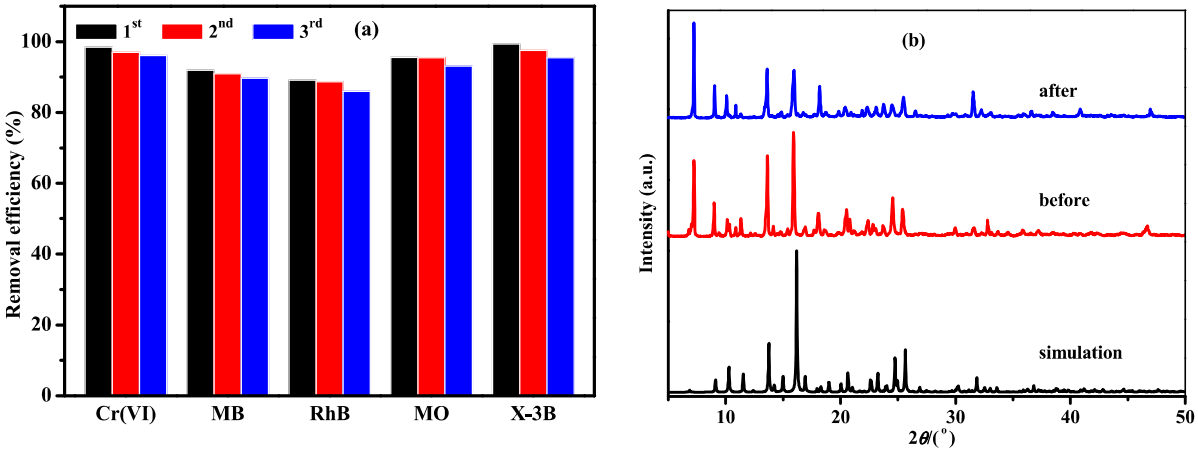

Fig. 9. (a) Cycling performance of the reduction of Cr(VI) and degradation of MB, RhB, MO and X-3B over **BUC-21**; (b) PXRD patterns of **BUC-21** before and after photocatalytic reaction and the simulated XRD pattern from the single-crystal structure of **BUC-21.**

sites present in the dyes, or the formation and stability of active intermediates responsible for decomposition, both of which are pH-dependent [79]. An alternative explanation is the greater concentration of hydroxide ions (OH^-) in the solution at higher pH, which induced the generation of hydroxyl free radicals (·OH) [80]. Under acidic conditions, ·OH played only a secondary role in decomposing X-3B (Fig. 7), probably because of its low concentration. However, at higher pH values, the degradation of X-3B was effectively promoted by the greater concentration of ·OH. In conclusion, **BUC-21** is stable (Fig. S3), and is especially effective towards organic pollutants across a wide range of pH from 2 to 12.

The recyclability and stability of **BUC-21** were tested by performing repeated usage cycles under identical reaction conditions. As shown in Fig. 9(a), the reduction rate of Cr(VI) over **BUC-21** stayed above 95%, and the removal of the four selected organic dyes showed only a small decrease, after three runs' photocatalytic reactions, indicating that **BUC-21** was highly stable and reusable. Moreover, the PXRD pattern of the used photocatalyst matched well with the simulated pattern based on the single-crystal data. It can be seen from Fig. 9(b) that the crystallographic structure and morphology of the catalyst underwent no noticeable change during the experiments, implying the good reusability and high stability of **BUC-21** for Cr(VI) reduction and dye decomposition.

The transient photocurrent responses of **BUC-21** under intermittent UV light irradiation are illustrated in Fig. 10, in which it is clear that **BUC-21** coated on FTO glass showed strong photocurrent responses, which rapidly decayed as soon as the light was switched off. These results indicate that **BUC-21** can be photoexcited to generate electron-hole pairs, which can then be separated efficiently, implying the good potential of **BUC-21** for practical use as a photocatalyst.

Most CPs and MOFs, with the exception of MOF-5 [81], belong to the class of molecular photocatalysts, whose mechanisms are usually explained in terms of frontier molecular orbital theory [7]. A possible mechanism for the photocatalytic reduction of Cr(VI) and degradation of organic dyes over **BUC-21** is proposed [7,82,83]. As illustrated in Fig. 4(b), under light irradiation, an electron (e^-) is excited from the highest occupied molecular orbital (HOMO) to the lowest unoccupied

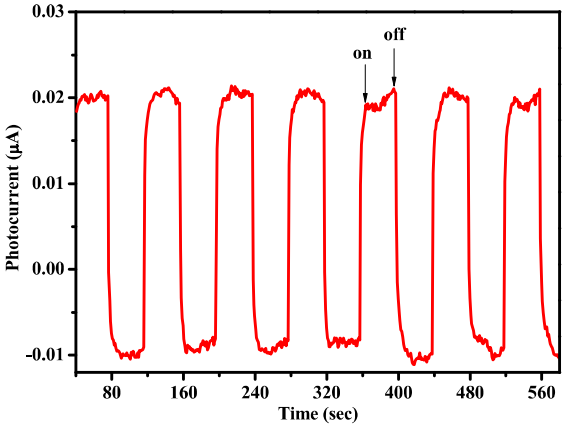

Fig. 10. Transient photocurrent response of **BUC-21** in Na_2SO_4 aqueous solution (0.2 mol L^{-1}) under UV light irradiation.

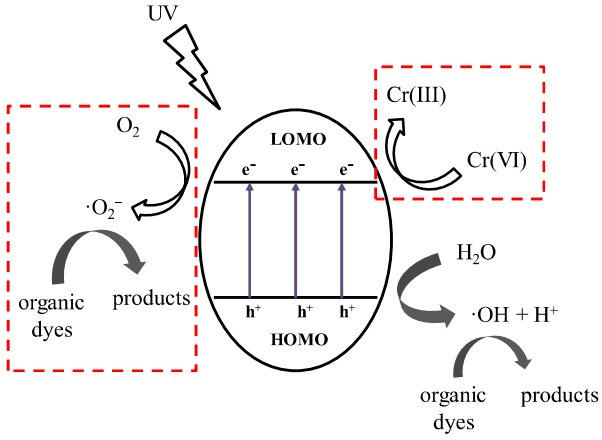

Fig. 11. A simplified model of the photocatalytic reaction mechanism in **BUC-21.**

molecular orbital (LUMO), producing a hole (h^+) in the former. The photo-induced electron in the LUMO is usually easily lost, and either takes part in the reduction of Cr(VI) to Cr(III), or is transferred to dissolved O_2 to generate $\cdot O_2^-$, which can then oxidize a dye molecule. The HOMO, however, strongly demands one electron to return to its stable state. Therefore, one electron is captured from a water molecule, which is oxygenated into ·OH. The ·OH radicals can further decompose organic dyes.

4. Conclusions

In summary, the synthesis of a new coordination polymer, **BUC-21**, has been accomplished. **BUC-21** exhibited excellent reusability, and much higher performance for photocatalytic reduction of Cr(VI) and degradation of dyes than P25 under UV light illumination. Moreover, the photocatalytic behavior of **BUC-21** in a mixed system of Cr(VI) and dye was also studied. In the mixed system, the reduction of Cr(VI) was not promoted, while the degradation of X-3B was significantly reduced, relative to the mono-component systems. The lower degradation rate of X-3B resulted from the consumption of photo-excited electrons by Cr(VI), limiting the generation of $\cdot O_2^-$, which was the main active species needed to decompose X-3B.

References

[1] W. L. Yang, Y. Liu, Y. Hu, M. J. Zhou, H. S. Qian, *J. Mater. Chem.*, **2012**, 22, 13895–13898.

[2] G. D. Chen, M. Sun, Q. Wei, Z. M. Ma, B. Du, *Appl. Catal. B*, **2012**, 125, 282–287.

[3] E. PetersonRoth, M. Reynolds, G. Quievryn, A. Zhitkovich, *Mol. Cell. Biol.*, **2005**, 25, 3596–3607.

[4] C. Liu, R. N. Jin, X. K. Ouyang, Y. G. Wang, *Appl. Surf. Sci.*, **2017**, 408, 77–87.

[5] A. M. Zayed, N. Terry, *Plant Soil*, **2003**, 249, 139–156.

[6] S. Pipileima, S. Ray, L. Menan Devi, R. Mohan B, G. Srinikethan, B.C. Meikap (Eds.) *Materials, Energy and Environment Engineering: Select Proceedings of ICACE 2015*, Springer Singapore, Singapore, **2017**, 137–144.

[7] C. C. Wang, J. R. Li, X. L. Lv, Y. Q. Zhang, G. S. Guo, *Energy Environ. Sci.*, **2014**, 7, 2831–2867.

[8] D. Z. Shen, J. X. Fan, W. Z. Zhou, B. Y. Gao, Q. Y. Yue, K. Qi, *J. Hazard. Mater.*, **2009**, 172, 99–107.

[9] C. C. Wang, X. D. Du, J. Li, X. X. Guo, P. Wang, J. Zhang, *Appl. Catal. B*, **2016**, 193, 198–216.

[10] L. A. M. Ruotolo, J. C. Gubulin, *Chem. Eng. J.*, **2009**, 149, 334–339.

[11] F. Rodriguez-Valadez, C. Ortiz-Exiga, J. G. Ibanez, A. Alatorre-Ordaz, S. Gutierrez-Granados, *Environ. Sci. Technol.*, **2005**, 39, 1875–1879.

[12] C. Barrera-Díaz, V. Lugo-Lugo, G. Roa-Morales, R. Natividad, S. A. Martínez-Delgadillo, *J. Hazard. Mater.*, **2011**, 185, 1362–1368.

[13] C. E. Barrera, *J. Hazard. Mater.*, **2012**, 223–224, 1–12.

[14] H. L. Ma, Y. W. Zhang, Q. H. Hu, D. Yan, Z. Z. Yu, M. L. Zhai, *J. Mater. Chem.*, **2012**, 22, 5914–5916.

[15] R. D. Ludwig, C. M. Su, T. R. Lee, R.T. Wilkin, S. D. Acree, R. R. Ross, A. Keeley, *Environ. Sci. Technol.*, **2007**, 41, 5299–5305.

[16] P. V. A. Padmanabhan, K. P. Sreekumar, T. K. Thiyagarajan, R. U. Satpute, K. Bhanumurthy, P. Sengupta, G. K. Dey, K. G. K. Warrier,

Graphical Abstract

Chin. J. Catal., 2017, 38: 2141–2149 doi: 10.1016/S1872-2067(17)62947-4

Photocatalytic Cr(VI) reduction and organic-pollutant degradation in a stable 2D coordination polymer

Fu-Xue Wang, Xiao-Hong Yi, Chong-Chen Wang *, Ji-Guang Deng *
Beijing University of Civil Engineering and Architecture; Beijing University of Technology

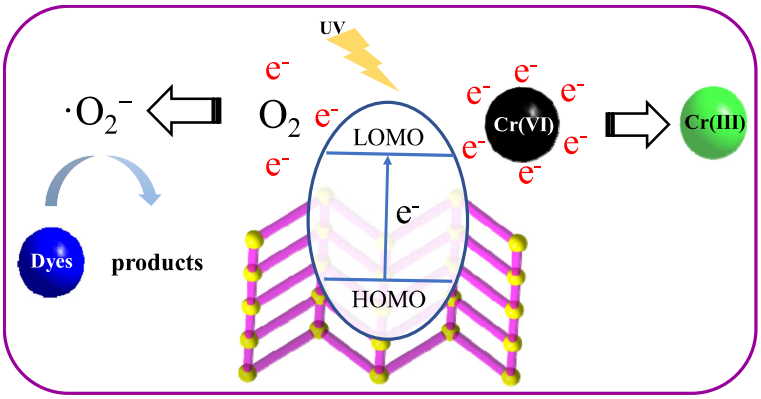

A novel 2D coordination polymer shows highly photocatalytic activities under UV light, which can reduce Cr(VI) to Cr(III) and decompose organic dyes effectively. Competition of photo-excited electron between Cr(VI) and organic dyes inhibited **BUC-21**'s photocatalytic activities in their matrix.

Vacuum, **2006**, 80, 1252–1255.
[17] J. J. Testa, M. A. Grela, M. I. Litter, *Environ. Sci. Technol.*, **2004**, 38, 1589–1594.
[18] L. M. Wang, N. Wang, L. H. Zhu, H. W. Yu, H. Q. Tang, *J. Hazard. Mater.*, **2008**, 152, 93–99.
[19] Z. H. Diao, X. R. Xu, D. Jiang, J. J. Liu, L. J. Kong, G. Li, L. Z. Zuo, Q. H. Wu, *Chem. Eng. J.*, **2017**, 315, 167–176.
[20] M. N. Chong, B. Jin, C. W. K. Chow, C. Saint, *Water Res.*, **2010**, 44, 2997–3027.
[21] H. Tong, S. X. Ouyang, Y. P. Bi, N. Umezawa, M. Oshikiri, J. H. Ye, *Adv. Mater.*, **2012**, 24, 229–251.
[22] X. J. Liu, L. K. Pan, T. Lv, G. Zhu, Z. Sun, C. Q. Sun, *Chem. Comm.*, **2011**, 47, 11984–11986.
[23] J. F. Qu, D. Y. Chen, N. J. Li, Q. F. Xu, H. Li, J. H. He, J. M. Lu, *Appl. Catal. B*, **2017**, 207, 404–411.
[24] L. X. Yang, Y. Xiao, S. H. Liu, Y. Li, Q. Y. Cai, S. L. Luo, G. M. Zeng, *Appl. Catal. B*, **2010**, 94, 142–149.
[25] W. Zhang, Y. B. Wang, Z. Wang, Z. Y. Zhong, R. Xu, *Chem. Comm.*, **2010**, 46, 7631–7633.
[26] H. H. Chen, X. Q. Xiong, L. L. Hao, X. Zhang, Y. M. Xu, *Appl. Surf. Sci.*, **2016**, 389, 491–495.
[27] P. Wang, Y. Sheng, F. Z. Wang, H. G. Yu, *Appl. Catal. B*, **2018**, 220, 561–569.
[28] Y. Lu, G. Liu, J. Zhang, Z. C. Feng, C. Li, Z. Li, *Chin. J. Catal.*, **2016**, 37, 349–358.
[29] K. L. He, J. Xie, X. Y. Luo, J. Q. Wen, S. Ma, X. Li, Y. P. Fang, X. C. Zhang, *Chin. J. Catal.*, **2017**, 38, 240–252.
[30] D. Z. Lu, W. Q. Chai, M. C. Yang, P. F. Fang, W. H. Wu, B. Zhao, R. Y. Xiong, H. M. Wang, *Appl. Catal. B*, **2016**, 190, 44–65.
[31] L. Shi, X. G. Meng, T. Wang, H. B. Zhang, K. Chang, H. M. Liu, J. H. Ye, *Adv. Sci.*, **2015**, 2, 1500006.
[32] M. A. Nasalevich, M. Van Der Veen, F. Kapteijn, J. Gascon, *CrystEngComm*, **2014**, 16, 4919–4926.
[33] A. M. Kirillov, Y. Y. Karabach, M. V. Kirillova, M. Haukka, A. J. L. Pombeiro, *Cryst. Growth Des.*, **2012**, 12, 1069–1074.
[34] M. Ranocchiari, J. A. van Bokhoven, *Phys. Chem. Chem. Phys.*, **2011**, 13, 6388–6396.
[35] S. Horike, Y. Inubushi, T. Hori, T. Fukushima, S. Kitagawa, *Chem. Sci.*, **2011**, 3, 116–120.
[36] Z. J. Li, J. Yao, Q. Tao, L. Jiang, T. B. Lu, *Inorg. Chem.*, **2013**, 52, 11694–11696.
[37] P. Kanoo, G. Mostafa, R. Matsuda, S. Kitagawa, T. K. Maji, *Chem. Commun.*, **2011**, 47, 8106–8108.
[38] A. C. Kizzie, A. G. Wong-Foy, A. J. Matzger, *Langmuir*, **2011**, 27, 6368–6373.
[39] B. Liu, H. Miao, L. Y. Pang, L. Hou, Y. Y. Wang, Q. Z. Shi, *CrystEngComm*, **2012**, 14, 2954–2958.
[40] R. J. Kuppler, D. J. Timmons, Q. R. Fang, J. R. Li, T. A. Makal, M. D. Young, D. Q. Yuan, D. Zhao, W. J. Zhuang, H. C. Zhou, *Coord. Chem. Rev.*, **2009**, 253, 3042–3066.
[41] J. J. Li, C. C. Wang, H. F. Fu, J. R. Cui, P. Xu, J. Guo, J. R. Li, *Dalton Trans.*, **2017**, 46, 10197–10201.
[42] X. D. Du, C. C. Wang, J. Zhong, J. G. Liu, Y. X. Li, P. Wang, *J. Environ. Chem. Eng.*, **2017**, 5, 1866–1873.
[43] D. Chisca, L. Croitor, E. B. Coropceanu, O. Petuhov, G. F. Volodina, S. G. Baca, K. Krämer, J. Hauser, S. Decurtins, S. X. Liu, M. S. Fonari, *Cryst. Growth Des.*, **2016**, 16, 7011–7024.
[44] L. P. Zhang, J. F. Ma, J. Yang, Y. Y. Pang, J. C. Ma, *Inorg. Chem.*, **2010**, 49, 1535–1550.
[45] J. Wang, Y. H. Zhang, H. X. Li, Z. J. Lin, M. L. Tong, *Cryst. Growth Des.*, **2015**, 7, 2352–2360.
[46] S. B. Wang, X. C. Wang, *Small*, **2015**, 11, 3097–3112.
[47] M. Rakibuddin, R. Ananthakrishnan, *Appl. Surf. Sci.*, **2016**, 362, 265–273.
[48] W. Y. Huang, N. Liu, X. D. Zhang, M. H. Wu, L. Tang, *Appl. Surf. Sci.*, **2017**, 425, 107–116.
[49] R. Y. Zhang, W. C. Wan, D. W. Li, F. Dong, Y. Zhou, *Chin. J. Catal.*, **2016**, 38, 313–320.
[50] L. J. Shen, R. W. Liang, L. Wu, *Chin. J. Catal.*, **2015**, 36, 2071–2088.
[51] H. M. Zhao, Q. S. Xia, H. Z. Xing, D. S. Chen, H. Wang, *ACS Sustain. Chem. Eng.*, **2017**, 5, 4449–4456.
[52] L. J. Shen, W. M. Wu, R. W. Liang, R. Lin, L. Wu, *Nanoscale*, **2013**, 5, 9374–9382.
[53] X. B. Wang, J. Liu, S. Leong, X. C. Lin, J. Wei, B. Kong, Y. F. Xu, Z. X. Low, J. F. Yao, H. T. Wang, *ACS Appl. Mater. Interfaces*, **2016**, 8, 9080–9087.
[54] J. X. Low, S. W. Cao, J. G. Yu, S. Wageh, *Chem. Comm.*, **2014**, 50, 10768–10777.
[55] Y. J. Cui, Y. X. Wang, H. Wang, F. Cao, F. Y. Chen, *Chin. J. Catal.*, **2016**, 37, 1899–1906.
[56] M. S. Akple, J. X. Low, Z. Y. Qin, S. Wageh, A. A. Al-Ghamdi, J. G. Yu, S. W. Liu, *Chin. J. Catal.*, **2015**, 36, 2127–2134.
[57] *Bruker AXS, SMART*, Version 5.611, Bruker AXS, Madison, WI, USA, **2000**.
[58] *Bruker AXS, SAINT*, Version 6.28, Bruker AXS, Madison, WI, USA, **2003**.
[59] *SADABS*, V2.03, Bruker AXS, Madison, WI, **2000**.
[60] G. M. Sheldrick, SHELX-97, Göttingen University, Germany, **1997**.
[61] X. L. Chen, B. Zhang, H. M. Hu, F. Fu, X. L. Wu, T. Qin, M. L. Yang, G. L. Xue, J. W. Wang, *Cryst. Growth Des.*, **2008**, 8, 3706–3712.
[62] T. Ma, M. X. Li, Z. X. Wang, J. C. Zhang, M. Shao, X. He, *Cryst. Growth Des.*, **2014**, 14, 4155–4165.
[63] C. G. Silva, A. Corma, H. García, *J. Mater. Chem.*, **2010**, 20, 3141–3156.
[64] J. L. Wang, C. Wang, W. B. Lin, *ACS Catal.*, **2012**, 2, 2630–2640.
[65] J. Guo, J. F. Ma, B. Liu, W. Q. Kan, J. Yang, *Cryst. Growth Des.*, **2011**, 11, 3609–3621.
[66] Y. Ku, I. L. Jung, *Water Res.*, **2001**, 35, 135–142.
[67] S. J. Yang, J. H. Im, T. Kim, K. Lee, C. R. Park, *J. Hazard. Mater.*, **2011**, 186, 376–382.
[68] J. Guo, J. Yang, Y. Y. Liu, J. F. Ma, *CrystEngComm*, **2012**, 14, 6609–6617.
[69] Z. Zhang, J. Yang, Y. Y. Liu, J. F. Ma, *CrystEngComm*, **2013**, 15, 3843–3853.
[70] Y. Park, Y. Na, D. Pradhan, B. K. Min, Y. Sohn, *CrystEngComm*, **2014**, 16, 3155–3167.
[71] X. H. Qi, Z. H. Wang, Y. Y. Zhuang, Y. Yu, J. L. Li, *J. Hazard. Mater.*, **2005**, 118, 219–225.
[72] T. Alammar, A. V. Mudring, *ChemSusChem*, **2011**, 4, 1796–1804.
[73] Y. Wu, J. Feng, B. Xie, L. K. Zou, Y. L. Li, Z. Q. Li, *J. Inorg. Organomet. Polym. Mater.*, **2017**, 27, 1243–1251.
[74] Z. H. Ai, J. L. Wang, L. Z. Zhang, *Chin. J. Catal.*, **2015**, 36, 2145–2154.
[75] X. Y. Tang, Z. C. Fan, C. Wen, Y. H. Hu, W. Y. Yin, H. J. Cheng, Y. S. Ma, R. X. Yuan, *Inorg. Chim. Acta*, **2016**, 451, 148–156.
[76] S. F. Li, X. Wang, Q. Q. He, Q. Chen, Y. L. Xu, H. B. Yang, M. M. Lü, F. Y. Wei, X. T. Liu, *Chin. J. Catal.*, **2016**, 37, 367–377.
[77] X. F. Hu, H. H. Ji, F. Chang, Y. M. Luo, *Catal. Today*, **2014**, 224, 34–40.
[78] S. G. Schrank, H. J. José, R. F. P. M. Moreira, *J. Photochem. Photobiol. A Chem.*, **2002**, 147, 71–76.
[79] X. Zhao, J. H. Qu , H. J. Liu, C. Hu, *Environ. Sci. Technol.*, **2007**, 41,

6802–6807.
[80] Y. S. Cao, J. X. Chen, L. Huang, Y. L. Wang, Y. Hou, Y. T. Lu, *J. Mol. Catal. A Chem.*, **2005**, 233, 61–66.
[81] M. Alvaro, E. Carbonell, B. Ferrer, F. X. Llabres Qi Xamera, H. Garcia, *Chem. Eur. J.*, **2007**, 13, 5106–5112.
[82] C. Gao, J. Wang, H. X. Xu, Y. J. Xiong, *Chem. Soc. Rev.*, **2017**, 46, 2799–2823.
[83] E. M. Dias, C. Petit, *J. Mater. Chem. A*, **2015**, 3, 22484–22506.

一种稳定二维配位聚合物用于光催化还原Cr(VI)及降解有机污染物

王茀学[a], 衣晓虹[a], 王崇臣[a,*], 邓积光[b,#]
[a]北京建筑大学, 建筑结构与环境修复功能材料北京重点实验室/中荷未来污水处理技术研究中心, 北京100044
[b]北京工业大学环境与能源工程学院, 化学与化工系, 北京100022

摘要: 工厂运行过程产生的大量含重金属离子和有机污染物的废水, 对环境和人体造成很大的危害. 光催化法是一种有效、无二次污染且成本较低的水处理技术，能将有机物分解为生化性强的小分子并降低毒性, 甚至完全矿化成二氧化碳和水；此外还能将剧毒的重金属转变为其它低毒或无毒形态，如可将Cr(VI)还原为Cr(III)，或将As(III)氧化为As(V). 传统的光催化剂往往面临效率低、重复性差等问题, 限制了其实际应用. 例如, 二氧化钛虽然廉价、毒性低，但巨大的比表面积能使其极易发生团聚，导致活性下降. 因此开发超高效光催化活性的催化剂具有重要意义.

本文利用水热法合成了一种新型配位聚合物Zn(bpy)L (**BUC-21**) (H_2L = 顺1,3-二苄基咪唑-2-酮-4,5-二羧酸, bpy=4, 4’-联吡啶). 对**BUC-21**进行了包括傅里叶变换红外光谱(FTIR)、热重(TGA)、CNH元素分析和紫外-可见漫反射(UV-vis DRS)在内的系列表征，并选择Cr(VI)和四种典型有机染料作为目标污染物探究了**BUC-21**的光催化性能.

结果表明, **BUC-21**在340 ºC以下时能保持骨架稳定, 其带隙值(E_g)为3.4 eV. 紫外光照射30 min后, **BUC-21**对Cr(VI)还原效率可达到96%, 远高于相同条件下的商业二氧化钛P25(39%). 此外, **BUC-21**还能高效降解亚甲基蓝(MB)、罗丹明B(Rh B)、甲基橙(MO)和活性红X-3B(X-3B)等有机染料污染物, 其降解速率同样优于P25. 比如，在紫外光照射下，P25完全降解X-3B需要21 min, 而**BUC-21**仅需9 min, 表明**BUC-21**具有比P25更好的光催化活性. 将**BUC-21**用于同时光催化还原Cr(VI)与降解X-3B反应, 结果表明, 较单一污染物组分而言，Cr(VI)还原效率不变而染料降解效率降低. 活性物质捕捉实验结果证明, 造成上述现象的原因在于Cr(VI)消耗了光生电子, 抑制超氧自由基($\cdot O_2^-$)的生成, 而$\cdot O_2^-$是降解X-3B的主要活性物质. 此外, **BUC-21**具有很好的耐酸耐碱性能, 能在pH值为2-12范围内保持稳定, 且表现出超高的光催化活性。循环实验表明, **BUC-21**具有良好的稳定性和重复利用性.

关键词: 光催化; Cr(VI)还原; 有机染料; 配位聚合物; 降解

收稿日期: 2017-10-04. 接受日期: 2017-10-26. 出版日期: 2017-12-05.

*通讯联系人. 电话/传真: (010)61209186; 电子信箱: chongchenwang@126.com
#通讯联系人. 电子信箱: jgdeng@bjut.edu.cn

基金来源: 国家自然科学基金(51578034); 北京自然科学基金重点项目暨北京市教委重点项目(KZ201410016018); 北京百千万人才工程培养经费(2016023); 北京市属高校高层次人才引进与培养计划及创新团队与教师职业发展计划 (IDHT20170508).
本文的电子版全文由Elsevier出版社在ScienceDirect上出版(http://www.sciencedirect.com/science/journal/18722067).